# On the Direct Detectability of the Cosmic Dark Ages: 21-cm Emission from Minihalos

Ilian T. Iliev[1], Paul R. Shapiro[2], Andrea Ferrara[1], and Hugo Martel[2]

## ABSTRACT

In the standard Cold Dark Matter (CDM) theory of structure formation, virialized minihalos (with $T_{\rm vir} \lesssim 10^4$ K) form in abundance at high redshift ($z > 6$), during the cosmic "dark ages." The hydrogen in these minihalos, the first nonlinear baryonic structures to form in the universe, is mostly neutral and sufficiently hot and dense to emit strongly at the 21-cm line. We calculate the emission from individual minihalos and the radiation background contributed by their combined effect. Minihalos create a "21-cm forest" of emission lines. We predict that the angular fluctuations in this 21-cm background should be detectable with the planned LOFAR and SKA radio arrays, thus providing a direct probe of structure formation during the "dark ages." Such a detection will serve to confirm the basic CDM paradigm while constraining the background cosmology parameters, the shape of the power-spectrum of primordial density fluctuations, the onset and duration of the reionization epoch, and the conditions which led to the first stars and quasars. We present results here for the currently-favored, flat ΛCDM model, for different tilts of the primordial power spectrum.

*Subject headings:* cosmology: theory — diffuse radiation — intergalactic medium — large-scale structure of universe — galaxies: formation — radio lines: galaxies

## 1. Introduction

No direct observation of the universe during the period between the recombination epoch at redshift $z \simeq 10^3$ and the reionization epoch at $z \gtrsim 6$ has yet been reported. While a number of suggestions for the future detection of the reionization epoch, itself, have been made, this period prior to the formation of the first stars and quasars – the cosmic "dark ages" – has been more elusive. Standard Big Bang cosmology in the CDM model predicts

[1]Osservatorio Astrofisico di Arcetri, Largo Enrico Fermi 5, 50125 Firenze, Italy

[2]Department of Astronomy, University of Texas, Austin, TX 78712

that nonlinear baryonic structure first emerges during this period, with virialized halos of dark and baryonic matter which span a range of masses from less than $10^4 M_\odot$ to about $10^8 M_\odot$ which are filled with neutral hydrogen atoms. The atomic density $n_H$ and kinetic temperature $T_K$ of this gas are high enough that collisions populate the hyperfine levels of the ground state of these atoms in a ratio close to that of their statistical weights (3:1), with a spin temperature $T_S$ that greatly exceeds the excitation temperature $T_* = 0.0681$K. Since, as we shall show, for the majority of the halos $T_S > T_{\rm CMB}$, the temperature of the Cosmic Microwave Background (CMB), as well, such "minihalos" can be a detectable source of redshifted 21-cm line emission.

The possibility of 21-cm line emission or absorption by neutral H at high redshift has been considered before (Hogan & Rees 1979; Scott & Rees 1990; Subramanian & Padmanabhan 1993; Kumar, Padmanabhan, & Subramanian 1995; Bagla, Nath, & Padmanabhan 1997; Madau, Meiksen & Rees 1997; Shaver, et al. 1999; Tozzi et al. 2000). Prior to the release of radiation by nonlinear baryonic structures which condense out of the background universe, the spin temperature of H I in the diffuse, uncollapsed gas in the intergalactic medium (IGM) is coupled to the CMB, so that $T_S = T_{\rm CMB}$ and neither emission nor absorption in the 21-cm line is possible. Recently, attention has focused on the possibility that radiation from early stars and quasars might decouple $T_S$ from $T_{\rm CMB}$ by "Ly$\alpha$ pumping" – resonant scattering in the H Ly$\alpha$ transition followed by decay of the upper state $n = 2$ to the ground state $n = 1$ into one or the other of the hyperfine levels (Madau et al. 1997; Tozzi et al. 2000). This mechanism, it has been suggested, will operate on H I in the diffuse, uncollapsed IGM during reionization, first to make $T_S < T_{\rm CMB}$, so that the 21-cm transition can be seen in *absorption* against the CMB, until the same Ly$\alpha$ scattering heats the gas shortly thereafter and makes $T_S > T_{\rm CMB}$, thereby causing 21-cm *emission* in excess of the CMB, before reionization finally destroys the H I. In what follows, however, we show that a substantial fraction of the baryons in the universe may already have condensed out of the diffuse IGM into virialized minihalos, *prior* to and during reionization. Under these conditions, collisional excitation alone is sufficient to decouple $T_S$ from $T_{\rm CMB}$ and cause 21-cm emission in excess of the CMB, thereby providing a signature of the cosmic "dark ages" and of their retreat during reionization.

## 2. 21-cm Emission from Individual Minihalos

The 21-cm emission from a single halo depends upon its internal atomic density, temperature, and velocity structure. We model each CDM minihalo here as a nonsingular, truncated isothermal sphere ("TIS") of dark matter and baryons in virial and hydrostatic equilibrium, in good agreement with the results of gas and N-body simulations from realistic initial conditions (Shapiro, Iliev & Raga 1999; Iliev & Shapiro 2001, 2002). This model uniquely specifies the internal structure of each halo (e.g. total and core sizes, $r_t$ and $r_0$, central total mass density $\rho_0$, dark matter velocity dispersion $\sigma_V = (4\pi\rho_0 r_0^2)^{1/2}$, and gas temperature $T_K = \mu m_p \sigma_V / k_B$, where $\mu$ is the mean molecular weight), for a given background cosmology as functions of two parameters, the total mass $M$ and collapse redshift $z_{\rm coll}$.

The minihalos which contribute significantly to the 21-cm emission span a mass range from $M_{\rm min}$ to $M_{\rm max}$ which varies with redshift. $M_{\rm min}$ is close to the Jeans mass of the uncollapsed IGM prior to reionization, $M_J = 5.7 \times 10^3\,(\Omega_0 h^2/0.15)^{-1/2} \times(\Omega_b h^2/0.02)^{-3/5}\,[(1+z)/10]^{3/2}\,M_\odot$, while $M_{\rm max} = 3.95\times 10^7(\Omega_0 h^2/0.15)^{-1/2}[(1+z)/10]^{-3/2}$ is the mass for which $T_{\rm vir} = 10^4$ K according to the TIS model (Iliev & Shapiro 2001) (since halos with $T_{\rm vir} \gtrsim 10^4$K are largely collisionally ionized). Halos with $T_{\rm vir} \gtrsim 10^4$K may have radiatively cooled gas inside them which would add to the signal we compute, but such gas is expected to lead to the formation of internal sources of ionizing radiation which will largely offset the effect. Since these additional effects are highly uncertain and are related to the onset of radiative feedback and reionization which we are neglecting in these calculations, we will not consider the role of higher temperature halos further.

The received flux per unit frequency, $\mathfrak{F}_\nu \equiv (dF/d\nu)_{\rm rec}$, at redshift $z=0$ at frequency $\nu_{\rm rec}$ from a minihalo at redshift $z$ which emits at frequency $\nu_{\rm em} = \nu_{\rm rec}(1+z)$ is expressed in terms of the brightness temperature $T_{b,\rm em} = T_{b,\rm rec}(1+z)$ according to

$$\mathfrak{F}_{\nu_{\rm rec}} = \frac{2\nu_{\rm rec}^2}{c^2} k_B T_{b,\rm rec} (\Delta\Omega)_{\rm halo}\,, \tag{1}$$

where $(\Delta\Omega)_{\rm halo} = \pi r_t^2/D_A^2 = \pi(\Delta\theta_{\rm halo}/2)^2$ is the solid angle subtended by the minihalo, and $D_A$ is the angular diameter distance. The brightness temperature $T_{b,\rm em}$ is determined by solving the equation of radiative transfer to derive the brightness profile of the minihalo and integrating this profile over the projected surface area, as follows.

The specific intensity along a line of sight thru the minihalo at projected distance $r$ from the center obeys the equation

$$I_\nu(r) = I_{0,\nu} e^{-\tau(r)} + \int_0^{\tau(r)} S_\nu e^{-\tau'} d\tau', \tag{2}$$

where $I_{0,\nu} = I_{\rm CMB}$ is the CMB intensity at the location of the minihalo, $\tau(r)$ is the total optical depth thru the halo along this line of sight, $S_\nu = j_\nu/\kappa_\nu$ is the source function, where $j_\nu$ and $\kappa_\nu$ are the 21-cm emissivity and absorption coefficient, respectively, and frequency $\nu$ refers here and henceforth to $\nu_{\rm em}$. The effective absorption coefficient $\kappa_\nu$ is given by:

$$\kappa_\nu = \frac{3c^2 A_{10} n_{\rm HI}}{32\pi\nu^2} f(\nu) \frac{T_*}{T_S} \tag{3}$$

(Field 1958), where $A_{10} = 2.85 \times 10^{-15}\mathrm{s}^{-1}$ is the Einstein $A$-coefficient for the 21-cm transition, $f(\nu)$ is the normalized line profile and we have used the fact that $T_* \ll T_S$.

The spin temperature $T_S$ which characterizes the level population of the 21-cm transition is determined by the balance between collisional and radiative excitation and de-excitation by atoms and electrons and by CMB and Ly$\alpha$ photons, respectively, according to

$$T_S = \frac{T_{CMB} + y_c T_K + y_\alpha T_\alpha}{1 + y_c + y_\alpha}\,, \tag{4}$$

where $T_\alpha$ is the color temperature of the Ly$\alpha$ photons, and $y_\alpha$ and $y_c$ are radiative and collisional excitation efficiencies, respectively (Purcell & Field 1956; Field 1958, 1959). The efficiency $y_c$ includes contributions from $\mathrm{H}^0 - \mathrm{H}^0$ collisions, $y_H$, and from $\mathrm{e}^- - \mathrm{H}^0$ collisions, $y_e$. Prior to the reionization epoch, Ly$\alpha$ pumping is unimportant and collisional excitation alone must compete with excitation by the CMB. This is only possible for gas that is highly nonlinear and sufficiently hot. Such conditions are achieved only inside virialized halos.

The optical depth of an individual halo is not negligible, particularly for smaller-mass halos (due to their lower $T_S$). We plot in Figure 1 (first panel) the optical depth at $\nu = \nu_0$, the line-central frequency 1420.41 MHz, along a line of sight through the halo center (i.e. at $r = 0$, where $\tau$ is maximum) as a function of the halo mass for several redshifts $1 + z = 7, 10, 15$, and 20.

From the principle of detailed balance and the definition of spin temperature, we obtain $S_\nu = B_\nu(T_S) = 2\nu^2 k_B T_S / c^2$, so the equation of transfer becomes

$$T_b(r) = T_{\mathrm{CMB}} e^{-\tau(r)} + \int_0^{\tau(r)} T_S e^{-\tau'} d\tau'\,, \tag{5}$$

where all quantities are defined in the comoving frame of the minihalo. Since $T_S$ varies with radial position inside the halo, as a result of its significant central concentration, we must integrate equation (5) numerically. The face-averaged $T_b$ of this single halo is given by $\langle T_b \rangle_{\mathrm{halo}} \equiv (\int T_b(r) dA)/A$, where $A(M, z)$ is the geometric cross-section of a halo of mass $M$ and collapse redshift $z$. The observed flux in the redshifted 21-cm line from an individual halo is then expressed with respect to the CMB by the differential antenna temperature:

$$\delta T_b = \frac{\langle T_b \rangle_{\mathrm{halo}} - T_{\mathrm{CMB}}(z)}{1 + z}. \tag{6}$$

The line-integrated flux $F(M, z)$ received from this minihalo is equal to the flux calculated for $\nu = \nu_0$ multiplied by a redshifted effective line-width $\Delta\nu_{\mathrm{eff}}(z)$, defined by $\Delta\nu_{\mathrm{eff}}(z) \equiv (\int \mathfrak{F} d\nu)/\mathfrak{F}_{\nu_0}$. For an optically thin minihalo, $\Delta\nu_{\mathrm{eff}}$ reduces to $\Delta\nu_{\mathrm{eff}}(z) = [f(\nu_0)(1+z)]^{-1}$. In that case, for a thermal-Doppler-broadened line profile, $\Delta\nu_{\rm eff}(z) = [(2\pi\mu)^{1/2}\nu_0\sigma_V/c](1+z)^{-1}$. We have checked that this approximation is adequate even for the optically thicker halos at the small-mass end of the mass function. The differential line-integrated flux $\delta F(M,z)$ is given by replacing $T_{b,\rm rec}$ in equation (1) by $\delta T_b$ from equation (6) and integrating over frequency as described above.

The resulting differential antenna temperature, total differential flux per unit frequency, and line-integrated flux, apparent angular size and observed line width are plotted against the mass of the minihalo for redshifts $1+z = 7, 10, 15$ and 20 in Figure 1. Line profiles of different minihalos along the same line of sight should not typically overlap. The proper mean free path $\lambda_{\rm mfp} = \langle n_{\rm halo}\sigma_{\rm halo}\rangle^{-1}$ for photons to encounter minihalos in $\Lambda$CDM is 160 kpc at $z = 9$ (Shapiro 2001), corresponding to a frequency separation, $\Delta\nu_{\rm sep} \approx \nu_0 H(z)\lambda_{\rm mfp}/[c(1+z)] \sim 0.1\,{\rm MHz} \gg \Delta\nu_{\rm eff} \lesssim 10\,{\rm kHz}$.

These results predict a "21-cm forest" of minihalo emission lines. At $z = 9$, for example, there are about 160 minihalo lines per unit redshift along a typical line of sight in an untilted $\Lambda$CDM universe (Shapiro 2001). Detecting the stronger lines would require sub-arcsecond spatial resolution, $\sim 1\,$kHz frequency resolution, and $\sim$ nJy sensitivity. SKA is expected to have sufficient resolution for such observation, but probably not sufficient sensitivity.

## 3. The Radiation Background from 21-cm Emission by Minihalos

The average differential flux per unit frequency relative to that of the CMB from all the minihalos observed within a given beam of angular size $\Delta\theta_{\rm beam}$ and frequency bin $\Delta\nu_{\rm obs}$ is:

$$\overline{\delta\mathfrak{F}}_\nu(z) = \frac{1}{\Delta\nu_{\rm obs}}\sum_{\rm beam}\delta F(M,z), \tag{7}$$

where the sum is over the solid angle $(\Delta\Omega)_{\rm beam} = \pi(\Delta\theta_{\rm beam}/2)^2$. We calculate the comoving density of halos at different redshifts using the Press-Schechter (PS) approximation for the halo mass function $dn/dM$. We consider the currently-favored, flat CDM model with cosmological constant ("$\Lambda$CDM", $\Omega_0 = 0.3$, $\lambda_0 = 0.7$, COBE-normalized, $\Omega_b h^2 = 0.02$, $h = 0.7$), for the three values of the primordial power spectrum index $n_p = 0.9$, 1, and 1.1, using fits to the primordial power spectrum from Eisenstein & Hu (1999) (for which $\sigma_8 = 0.96$). The average differential flux per unit frequency from equation (7) becomes:

$$\overline{\delta\mathfrak{F}}_\nu(z) = \frac{\Delta z(\Delta\Omega)_{\rm beam}}{\Delta\nu_{\rm obs}}\frac{d^2V(z)}{dz\,d\Omega}\int_{M_{\rm min}}^{M_{\rm max}}\left(\delta F\frac{dn}{dM}\right)(M,z)dM, \tag{8}$$

where $d^2V(z)/dz\,d\Omega$ is the comoving volume per unit redshift per unit solid angle. If we define the beam-averaged "effective" differential antenna temperature $\overline{\delta T_b}$ using $\overline{\delta\mathfrak{F}}_\nu =$

$2\nu^2 k_B \overline{\delta T_b} (\Delta\Omega)_{\rm beam}/c^2$, then

$$\overline{\delta T}_b = \frac{c(1+z)^4}{\nu_0 H(z)} \int_{M_{\rm min}}^{M_{\rm max}} \left(\Delta\nu_{\rm eff}\delta T_b A \frac{dn}{dM}\right)(M,z)dM, \tag{9}$$

where we have used $\Delta\nu_{\rm obs}/\Delta z = \nu_0/(1+z)^2$.

The results for $\overline{\delta\mathfrak{F}}_\nu$ and $\overline{\delta T}_b$ are plotted in Figure 2. In principle, the variation of $\overline{\delta T_b}$ with observed frequency implied by the redshift variations in Figure 2 should permit a discrimination between the 21-cm emission from minihalos and the CMB and other backgrounds, due to their very different frequency dependences. If so, then it is interesting that even small differences in the tilt index $n_p$ from the Harrison-Zel'dovich value $n_p = 1$ which are consistent with current observational constraints can be distinguished by the frequency spectrum of the 21-cm background. However, the average differential brightness temperature of this minihalo background is very low and its evolution is fairly smooth, so such measurement may be difficult in practice with currently planned instruments like LOFAR and SKA. The angular fluctuations in this emission, on the other hand, should be much easier to detect, as discussed in the next section.

## 4. Angular Fluctuations in the 21-cm Emission Background

The amplitude of $q$-$\sigma$ angular fluctuations (i.e. $q$ times the rms value) in the differential antenna temperature is given in the linear regime by

$$\frac{\langle \delta T_b^2 \rangle^{1/2}}{\overline{\delta T_b}} = q b(z) \sigma_p, \tag{10}$$

where $\sigma_p$ is the rms mass fluctuation at redshift $z$ in a randomly placed cylinder which corresponds to the observational volume defined by the detector angular beam size, $\Delta\theta_{\rm beam}$, and frequency bandwidth, $\Delta\nu_{\rm obs}$, and $b(z)$ is the bias factor which accounts for the clustering of rare density peaks relative to the mass. We assume $b(z)$ is the flux-weighted average over the mass function of $b(M,z) = 1 + (\nu_{\rm h}^2 - 1)/\delta_c$, the linear bias factor, where $\nu_{\rm h} = \delta_c/\sigma(M)$, $\delta_c$ is the value of the linearly extrapolated value of overdensity $\delta\rho/\rho$ corresponding to the epoch when a top-hat collapse reaches infinite density, and $\sigma(M)$ is the the standard deviation of the density contrast filtered on mass scale $M$ (e.g. Mo & White 1996). For a cylinder of comoving radius $R = \Delta\theta_{\rm beam}(1+z)D_A(z)/2$, and length $L \approx (1+z)cH(z)^{-1}(\Delta\nu/\nu)_{\rm obs}$, we have :

$$\begin{aligned} \sigma_p^2 &= \frac{8D^{-2}(z)}{\pi^2 R^2 L^2} \int_0^\infty dk \int_0^1 dx \frac{\sin^2(kLx/2) J_1^2[kR(1-x^2)^{1/2}]}{x^2(1-x^2)} \\ &\quad \times (1+fx^2)^2 \frac{P(k)}{k^2} \end{aligned} \tag{11}$$

(Tozzi et al. 2000) (with several typos in the corresponding expression in that paper corrected here), where $D(z) \equiv \delta_+(0)/\delta_+(z)$ is the linear growth factor, $P(k)$ is the linear power spectrum at $z = 0$, and the factor $(1 + fx^2)^2$, with $f \approx [\Omega(z)]^{0.6}$, is the correction to the cylinder length for the departure from Hubble expansion due to peculiar velocities (Kaiser 1987).

Illustrative results are plotted in Figure 3 for 3-$\sigma$ fluctuations as a function of $\Delta\theta_{\rm beam}$, for $z = 8.5$ and bandwidth $\Delta\nu_{\rm obs} = 1$ MHz, along with the expected sensitivity limits for the planned LOFAR (300 m filled aperture) and SKA (1 km filled aperture) arrays, for a confidence level of 5 times the noise level obtained after the corresponding integration time. These 3-$\sigma$ fluctuations should be observable with both LOFAR and SKA with integration times $\gtrsim$ 100 hours.

We plot in Figure 4 the predicted spectral variation of these fluctuations vs. redshift $z$ for an illustrative beam size of $\Delta\theta_{\rm beam} = 25'$, along with the predicted sensitivities for LOFAR and SKA, for integration times of 100 h and 1000 h, for the compact subaperture, assuming rms sensitivity $\propto \nu^{-2.4}$, which is a good fit to the dependence according to the LOFAR design specifications. For such a beam size, 3-$\sigma$ fluctuations can be detected for untilted ΛCDM with a 100 h integration for $z \sim 6 - 11$ and a 1000 h integration for $z \lesssim 16$. Results for different values of $z$ and $\Delta\theta_{\rm beam}$ are available upon request.

## Acknowledgments

We are grateful to E. Scannapieco for clarifying the effects of bias. This work was supported in part by European Community RTN contract HPRN-CT2000-00126 RG29185 and grants NASA ATP NAG5-10825 and NAG5-10826 and Texas Advanced Research Program 3658-0624-1999.

## REFERENCES

Bagla, J. S., Nath, B., & Padmanabhan, T. 1997, MNRAS, 289, 671

Field, G. B. 1958, Proc. I.R.E., 46, 240

Field, G. B. 1959, ApJ, 129, 536

Eisenstein, D. J., & Hu, W. 1999, ApJ, 511, 5

Hogan, C. J., & Rees, M. J. 1979, MNRAS, 188, 791

Iliev, I. T., & Shapiro, P. R. 2001, MNRAS, 325, 468

Iliev, I. T., & Shapiro, P. R. 2002, in "The Mass of Galaxies at Low and High Redshift" (ESO Astrophysics Symposia), eds. R. Bender & A. Renzini (Heidelberg: Springer-Verlag), in press (astro-ph/0112427)

Kaiser, N. 1987, MNRAS, 227, 1

Kumar, A., Padmanabhan, T., & Subramanian, K. 1995, MNRAS, 272, 544

Madau, P., Meiksen, A., & Rees, M. J. 1997, ApJ, 475, 429

Mo, H., & White, S. D. M. 1996, MNRAS, 282, 347

Purcell, E. M., & Field, G. B. 1956, ApJ, 124, 542

Scott, D., & Rees, M. J. 1990, MNRAS, 247, 510

Shapiro, P. R. 2001, in Proceedings of the 20th Texas Symposium on Relativistic Astrophysics and Cosmology, eds. H. Martel and J. C. Wheeler, (AIP Conference Series), pp. 219-232

Shapiro, P. R., Iliev, I. T., & Raga, A. C. 1999, MNRAS, 307, 203

Shaver, P. A., Windhorst, R. A., Madau, P., & de Bruyn, A. G. 1999, A&A, 345, 390

Subramanian, K., & Padmanabhan, T. 1993, MNRAS, 265, 101

Tozzi, P., Madau, P., Meiksen, A., & Rees, M. J. 2000, ApJ, 528, 597

Fig. 1.— Individual minihalo sources of redshifted 21-cm emission in ΛCDM, redshifts $1+z=7$ (short-dashed line), 10 (solid line), 15 (long-dashed line), and 20 (dotted line) vs. total mass of minihalo $M$. From top to bottom: optical depth $\tau_{\nu_0}(r=0)$ at line-centered frequency $\nu_0$ thru minihalo center, differential antenna temperature $\delta T_b$, line-integrated differential flux $\delta F(M,z)$ relative to the CMB, total differential flux per unit frequency $\mathfrak{F}_\nu$, angular size of minihalo $(\Delta\theta)_{\rm halo}$, and redshifted effective width $\Delta\nu_{\rm eff}(z)$ of the 21-cm line as observed at $z=0$ at received frequency $\nu_{\rm rec}=\nu_0(1+z)^{-1}$.

Fig. 2.— Minihalo radiation background. Average observed differential antenna temperature $\overline{\delta T_b}$ and average differential flux per unit frequency $\overline{\delta\mathfrak{F}_\nu}$ for beam size of $\Delta\theta_{\rm beam}=10'$ at

---

the redshifted 21-cm line frequency due to minihalos vs. redshift $z$ for ΛCDM models with power-spectrum tilts $n_p = 0.9$, 1.0, and 1.1, as labelled.

Fig. 3.— Predicted 3-$\sigma$ differential antenna temperature fluctuations at $z = 8.5$ ($\nu_{\rm rec} = 150$ MHz) vs. angular scale $\Delta\theta$ for ΛCDM models with tilt $n = 0.9$, 1.0, and 1.1, as labelled (solid curves). Also indicated is the predicted sensitivity of LOFAR and SKA integration times of 100 h (dashed lines) and 1000 h (dotted lines), with compact subaperture (horizontal lines) and extended configuration needed to achieve higher resolution (diagonal lines) (see http://www.lofar.org/science).

Fig. 4.— Predicted 3-$\sigma$ differential antenna temperature fluctuations at $\Delta\theta_{\rm beam} = 25'$ vs. redshift $z$ for for ΛCDM models with tilt $n = 0.9$, 1.0, and 1.1, as labelled (solid curves). Also indicated is the predicted sensitivity for integration times 100 h (dashed curve) and 1000 h (dotted curve) of either LOFAR or SKA, for compact subaperture and assuming rms sensitivity $\propto \nu^{-2.4}$ (see http://www.lofar.org/science).

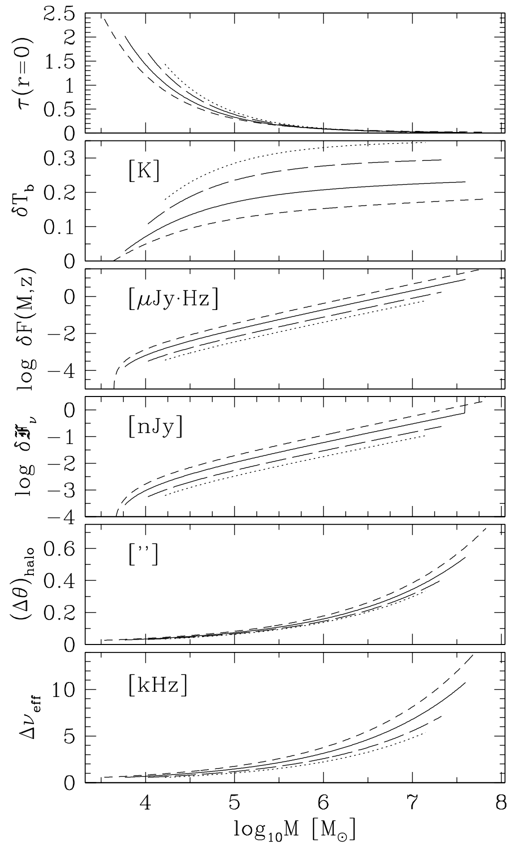

$\tau$(r=0)
$\delta T_b$
[K]
log $\delta$F(M,z)
[$\mu$Jy·Hz]
log $\delta\mathfrak{F}_\nu$
[nJy]
$(\Delta\theta)_{halo}$
['']
$\Delta\nu_{eff}$
[kHz]
$\log_{10}$M [$M_\odot$]


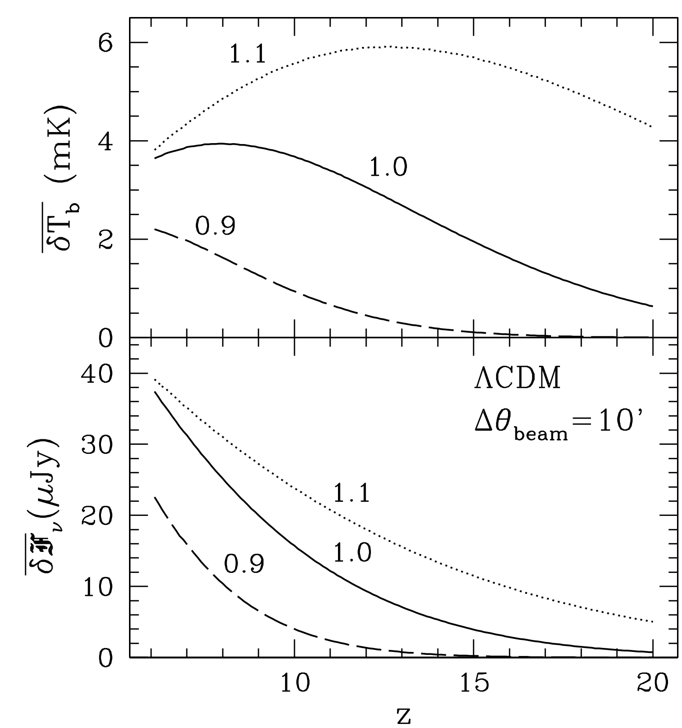

$\overline{\delta T_b}$ (mK)
1.1
1.0
0.9
$\overline{\delta\mathfrak{F}}_\nu(\mu Jy)$
ΛCDM
$\Delta\theta_{beam}$=10'
z

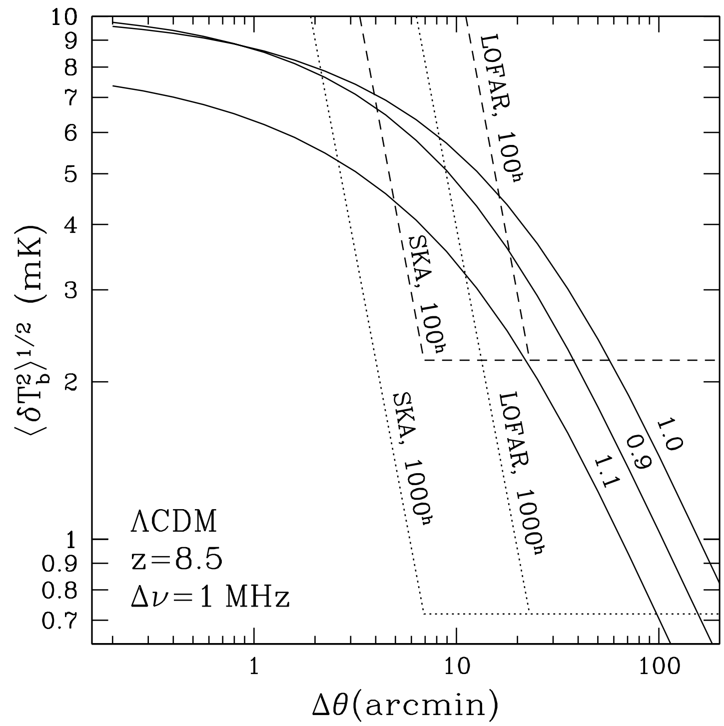

LOFAR, 100h
SKA, 100h
SKA, 1000h
LOFAR, 1000h
1.0
0.9
1.1
ΛCDM
z=8.5
Δν=1 MHz
Δθ(arcmin)
⟨δT_b^2⟩^{1/2} (mK)


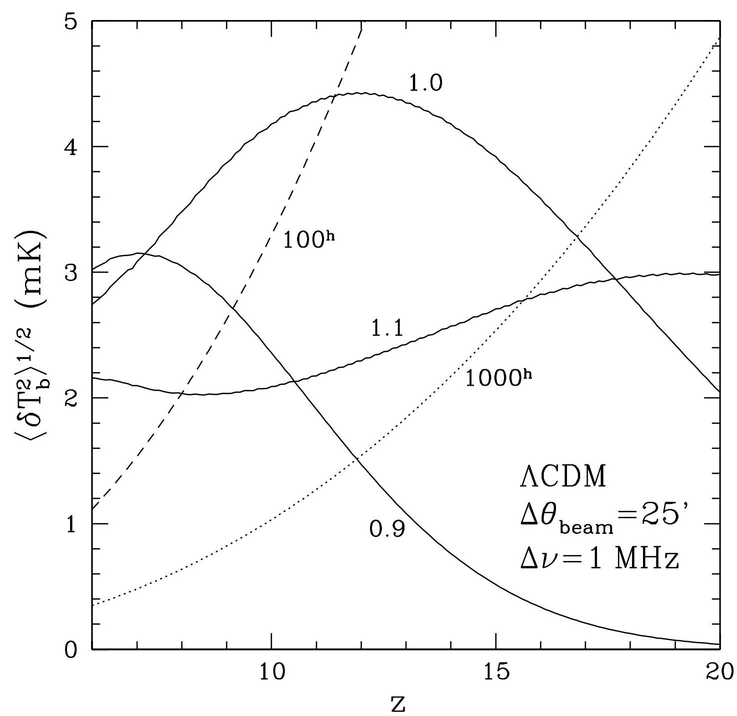

1.0
100h
1.1
1000h
0.9
ΛCDM
Δθ_beam=25'
Δν=1 MHz
z
⟨δT_b^2⟩^{1/2} (mK)